Available online at www.sciencedirect.com
SCIENCE DIRECT
Thermochimica Acta 447 (2006) 13–21
thermochimica acta
www.elsevier.com/locate/tca

Non-isothermal crystallization kinetics of poly(trimethylene terephthalate)/poly(ethylene 2,6-naphthalate) blends

Mingtao Run *, Yingjin Wang, Chenguang Yao, Jungang Gao

College of Chemistry & Environmental Science, Hebei University, Baoding 071002, China

Received 21 January 2006; received in revised form 10 April 2006; accepted 10 April 2006
Available online 27 April 2006

Abstract

The glass-transition temperature and non-isothermal crystallization of poly(trimethylene terephthalate)/poly(ethylene 2,6-naphthalate) (PTT/PEN) blends were investigated by using differential scanning calorimeter (DSC). The results suggested that the binary blends showed different crystallization and melting behaviors due to their different component of PTT and PEN. All of the samples exhibited a single glass-transition temperature, indicating that the component PTT and PEN were miscible in amorphous phase. The value of T_g predicted well by Gordon–Taylor equation decreased gradually with increasing of PTT content. The commonly used Avrami equation modified by Jeziorny, Ozawa theory and the method developed by Mo were used, respectively, to fit the primary stage of non-isothermal crystallization. The kinetic parameters suggested that the PTT content improved the crystallization of PEN in the binary blend. The crystallization growth dimension, crystallization rate and the degree of crystallinity of the blends were increased with the increasing content of PTT. The effective activation energy calculated by the advanced iso-conversional method developed by Vyazovkin also concluded that the value of E_a depended not only on the system but also on temperature, that is, the binary blend with more PTT component had higher crystallization ability and the crystallization ability is increased with increasing temperature. The kinetic parameters U^* and K_g were also determined, respectively, by the Hoffman–Lauritzen theory.

Keywords: Poly(trimethylene terephthalate); Poly(ethylene 2,6-naphthalate); Non-isothermal crystallization kinetics; Binary blends; Effective activation energy

1. Introduction

Poly(trimethylene terephthalate) (PTT) was first patented by Whinfield and Dickson [1] in 1946 and commercial produced by Shell Chemicals until the 1990s. Many properties of PTT are between those of poly(ethylene terephthalate) (PET) and poly(butylene terephthalate) (PBT), such as crystallization rate and glass transition temperature. Moreover, it combines the two key advantages of PET and PBT into one polymer, and it has an important application in the textile industry [2] and as a promising engineering thermoplastic [3]. Poly(ethylene 2,6-naphthalate) (PEN), featuring a molecular structure of a naphthalene ring instead of the benzene ring in PET, is used as a high-performance polymer and that has superior strength, heat stability, and barrier properties due to its increased chain stiffness [4]. Thus, PEN has found for a variety of applications, such as tire cords of automobiles [5] and base films of videotapes [6–8], etc.

Polymer blending is an attractive alternative for producing new polymeric materials with desirable properties without having to synthesize a totally new material. Other advantages for polymer blending are versatility, simplicity, and inexpensiveness. Due to the similarity in the chemical structure of these linear aromatic polyesters, numerous research works related to various aspects of polyesters' blends are available in the reported literatures. Blends of polyesters were investigated wildly, such as PEN and poly(butylene 2,6-naphthalate) (PBN) [9]; PET and PBT [10]; PET and PEN [11]; PTT and PET [12]; PTT and PBT [13]; and PTT and PEN [14], etc. To meet the growing demands of the plastics industry, the combination of the economics of PTT and the superior properties of PEN may become very important.

Recently, Supaphol [14] studied the miscibility, melting and crystallization behavior of PTT/PEN blends. PTT and PEN were miscible in the amorphous state in all of the blends compositions studied, as evidenced by a single, composition-dependent glass transition temperature (T_g) observed for each

* Corresponding author. Tel.: +86 312 2234679; fax: +86 312 5079525.
E-mail address: rmthyp@hotmail.com (M. Run).

0040-6031/$ – see front matter © 2006 Elsevier B.V. All rights reserved.
doi:10.1016/j.tca.2006.04.005

blend composition. The variation in the T_g value with the blend composition was well predicted by the Gordon–Taylor equation, with the fitting parameter being 0.57. The cold-crystallization peak temperature decreased with increasing PTT content, while the melt-crystallization peak temperature decreased with increasing amount of the minor component. The subsequent melting behavior after both cold- and melt-crystallization exhibited melting point depression, in which the observed melting temperatures decreased with increasing amount of the minor component. During melt-crystallization, both components in the blends crystallized concurrently just to form their own crystals. The blend with 60% (w/w) of PTT exhibited the lowest total apparent degree of crystallinity.

Studies related to the kinetics of polymer crystallization are of great importance in polymer processing, due to the fact that the resulting physical properties are strongly dependent on the morphology formed and the extent of crystallization occurring during processing. In the present study, blends of PTT and PEN were prepared and characterized for their non-isothermal crystallization kinetics and melting behavior by using DSC measurements. The objectives for this work are: (1) to investigate the effect of blend composition on melt-crystallization and melting behavior, (2) to investigate the effect of blend composition on non-isothermal crystallization kinetics, and (3) to assess the effect of the cooling rate on the crystallization behavior of the binary blend.

2. Experimental

2.1. Materials

The PTT homopolymer was supplied in pellet form by Shell Chemicals (USA) with an intrinsic viscosity of 0.92 dL/g measured in a phenol/tetrachloroethane solution (60/40, w/w) at 25 °C. The PEN homopolymer was supplied in pellet form by Honeywell (USA) with an intrinsic viscosity of 0.89 dL/g measured in phenol/tetrachloroethane solution (50/50, w/w) at 30 °C.

2.2. Blends preparation

The materials were dried in a vacuum oven at 140 °C for 12 h before preparing blends. The dried pellet of PTT and PEN were mixed together with different weight ratio of PTT/PEN as following: B1, 0/100; B2, 20/80; B3, 40/60; B4, 60/40; B5, 80/20; B6, 100/0, and then melt-blended in a ZSK-25WLE WP self-wiping, co-rotating twin-screw extruder, operating at a screw speed of 60 rpm and at a die temperature of 300 °C. The resultant blend ribbons were cooled in cold water, cut up, re-dried before being used in DSC.

2.3. Differential scanning calorimetry (DSC)

The glass-transition temperature, cold crystallization, and subsequent melting behavior of six samples were studied by the Perkin-Elmer Diamond DSC instrument that calibrated with indium prior to performing the measurement, and the weights of all samples were approximately 6 mg. The samples were heated to 300 °C at 150 °C/min under a nitrogen atmosphere, held for 5 min to reset previous thermal histories, after which all of the samples were immediately quenched under a cooling rate of 200 °C/min to obtain the completely amorphous state of six samples, and then heated them with a heating rate of 10 °C/min.

The melt-crystallization and subsequent melting behaviors of various binary blends were performed as following: the samples were heated to 300 °C at 150 °C/min under a nitrogen atmosphere, held for 5 min and then cooled to 50 °C at a constant cooling rate of 10 °C/min, and then heated them to 300 °C at a heating rate of 10 °C/min, the cooling process and the second heating process were recorded, respectively.

The non-isothermal crystallization behaviors of two blends (B2 and B3) were performed as following: the sample was heated to 300 °C in nitrogen, held for 5 min and then cooled to 50 °C at constant cooling rates of 5, 10, 15, and 20 °C/min, respectively. It is worth noting that each sample was used only once and its weight is around 6 ± 0.5 mg. The exothermic curves of heat flow as a function of temperature were recorded and investigated.

3. Results and discussion

3.1. Miscibility of the blends

Generally, a single T_g and/or its shift in the blends represent miscibility or partial miscibility [15–17]. In our experiment, all the blends are thought to be miscible in the amorphous phase. This is in good agreement with the report of Krutphun and Supaphol [14]. Fig. 1 displays the DSC curves of glass transition, cold-crystallization and subsequent melting for quenched six samples recorded with a heating rate of 10 °C/min. The dependence of T_g on the blend composition can be predicted by the Gordon–Taylor [18] and Fox [19] equations. In this paper, Gordon–Taylor equation is employed to describe the relationship between T_g and blend composition, and the result is shown

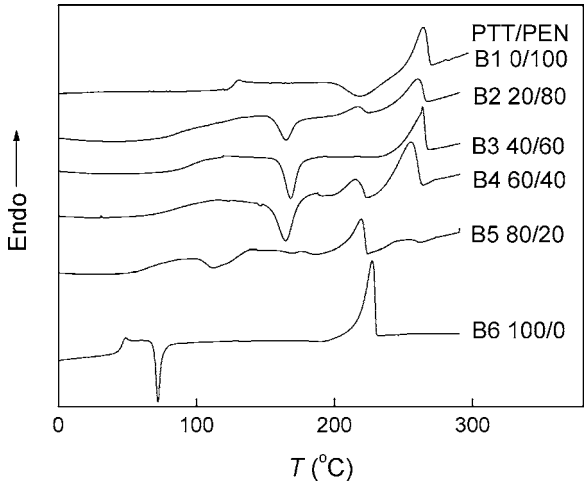

Fig. 1. The glass-transition temperature, cold-crystallization, and subsequent melting thermograms of six quenched samples under a heating rate of 10 °C/min.

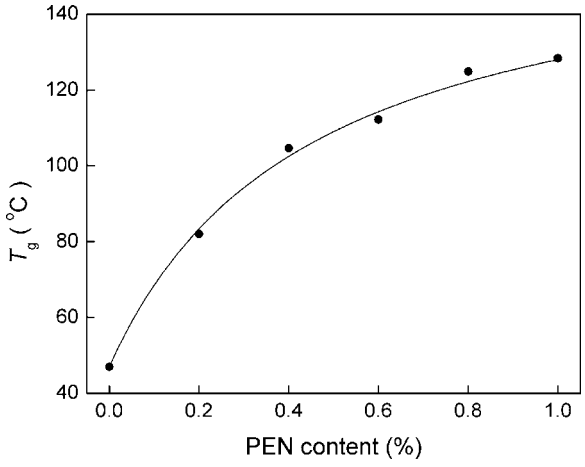

Fig. 2. T_g values of six samples as a function of blend composition. The solid line represents fits of the Gordon–Taylor equation.

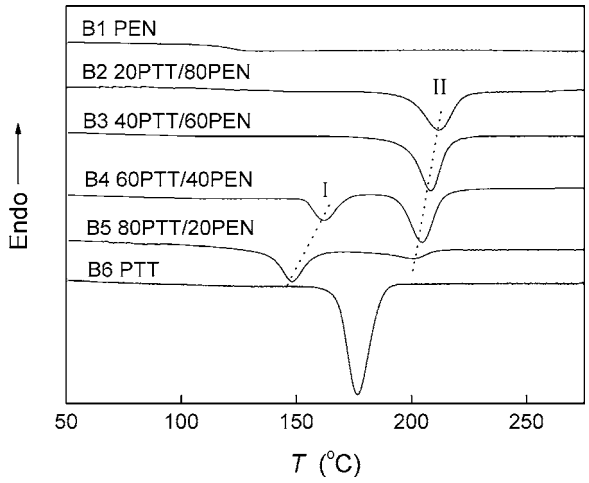

Fig. 3. DSC melt-crystallization curves of six samples at the cooling rate of 10 °C/min.

in Fig. 2.

$$T_g = \frac{w_1 T_{g1} + k w_2 T_{g2}}{w_1 + k w_2} \quad (1)$$

where w_1 and w_2 are the weight fractions of the components of PTT and PEN, respectively. T_{g1} and T_{g2} are the values of the pure components PTT and PEN, respectively. The parameter k is adjustable and the fitting value is 0.31.

From Figs. 1 and 2, it is apparent that a single T_g is observed in each curve, and the T_g values of the B2–B5 blends are observed between those of pure components (T_{gPTT} = 47 °C and T_{gPEN} = 128 °C). The T_g of each blend clearly shifts to higher temperature with increasing of PEN component. The result suggests clearly that PTT and PEN are complete miscibility in amorphous phase at all blend compositions.

3.2. Melt-crystallization and subsequent melting behavior

Fig. 3 shows the DSC curves of six samples with various PTT content at a given cooling rate and the crystallization parameters are listed in Table 1. According to Fig. 3 and Table 1, an apparent exotherm is observed for PTT with a crystallization peak temperature (T_p) at 186.7 °C, while none crystallization exotherm of the pure PEN is seen under the same cooling rate of 10 °C/min. This result suggests that PTT with flexible molecular chains is more crystallizable than PEN with chain stiffness, and the crystallization for PEN is almost inhibited at this cooling rate.

For B2 and B3 blends, each curve is shown with only one crystallization exothermic peak at higher temperature, indicating that the molecular chains of PEN can crystallize at the cooling rate of 10 °C/min as PTT component existing in the blend melt. While no exothermic peak is observed at lower temperature which may corresponding to the crystallization of PTT in the DSC curve, suggesting that the crystallization behavior of PTT component is inhibited by the major component of PEN although the weight percentage of PTT are 20% (w/w) in B2 and 40% (w/w) in B3. In these two binary blends, the melt viscosity of PEN is lowered by PTT component; therefore, molecular chains of PEN can crystallize at higher temperature with growth rates.

However, the exotherms of B4 and B5 blends exhibit two main crystallization peaks: the peak II at higher temperature and peak I at lower temperature, which may be attributed to the crystallization of PEN and PTT, respectively. The result suggests that both PTT and PEN components in the blends crystallized individually when the PTT become the major component. By careful observation, it is easy to found that the T_{pII} values of PEN component in blends decrease monotonically with the decreasing amount of the PEN component, suggesting that the crystallization behavior of the PEN component in the blends is relevant to its amount. On the other hand, the T_{pI} of B4 and B5 are lower

Table 1
Parameters of PTT/PEN blends during melt-crystallization and subsequent melting process

Samples	Crystallization process				Melting process		
	T_{onset} (°C)	T_{pI} (°C)	T_{pII} (°C)	ΔH_c (J/g)	T_{mI} (°C)	T_{mII} (°C)	ΔH_m (J/g)
B1 PEN	–	–	–	–	–	–	–
B2 20PTT/80PEN	220.6	–	211.6	−31.6	–	264.9	38.0
B3 40PTT/60PEN	215.6	–	208.3	−37.9	–	262.4	42.5
B4 60PTT/40PEN	213.9	162.0	204.6	−31.1	219.2	257.0	38.5
B5 80PTT/20PEN	206.6	148.3	201.4	−28.1	222.5	253.5	43.9
B6 PTT	186.7	176.7	–	−50.5	225.5	–	65.9

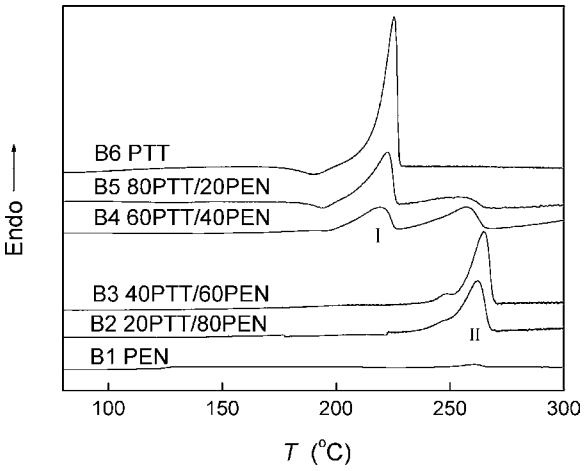

Fig. 4. DSC melting thermograms of six samples at the heating rate of 10 °C/min.

than that of pure PTT, suggesting that the crystallization of PTT component may be retarded by the PEN crystals that have been formed at higher temperature.

A series of DSC thermograms of six samples after melt-crystallization are shown in Fig. 4 and the melting parameters are also listed in Table 1. It is seen clearly from Fig. 4 that the melting thermograms for B6 (PTT) sample exhibits a single endotherm peak with the value of T_m at 225.5 °C. While in the DSC curve of B1 (PEN), none melting peak is shown resulting from none of the crystals formed in the melt-crystallization process. For each blend of B2 and B3, one sharp melting peak can be observed at higher temperature, 264.9 and 262.4 °C, respectively. These melting peaks should correspond to the melting behavior of PEN component. However, none melting peak is observed at lower temperature due to none of the crystals of PTT component formed in the melt-crystallization process. From both melting curves of B4 and B5, it can be easily found two exothermic peaks, T_{mI} and T_{mII}, which are corresponding to the melting of the crystals of PTT and PEN components, respectively. Moreover, the melting behavior of the PEN component in PEN-rich blends exhibits the usually observed multiple-melting phenomenon [20,21].

By careful observation, it is easy to found that the values of melting peak of the PEN component decrease with increasing of the PTT component. When certain blends are miscible, melting point depression is a fundamental phenomenon in characterizing the corresponding blends [21–24]. In general, thermodynamic considerations predict that the chemical potential decreases with the addition of miscible diluents. When one component is crystallizable, its decrease in chemical potential leads to a decreasing of the melting point [24].

3.3. Non-isothermal crystallization kinetics analysis

3.3.1. Analysis based on the Avrami theory modified by Jeziorny

The relative crystallinity (X_t) as a function of temperature is defined as the following equation:

$$X_t = \frac{\int_{t_0}^{t}(\mathrm{d}H/\mathrm{d}t)\,\mathrm{d}t}{\int_{t_0}^{t_\infty}(\mathrm{d}H/\mathrm{d}t)\,\mathrm{d}t} = \frac{A_0}{A_\infty} \tag{2}$$

where the $\mathrm{d}H/\mathrm{d}t$ is the rate of heat evolution, t_0 and t_∞ are the time, at which crystallization starts and ends of the crystallization process, and A_0 and A_∞ are areas under the normalized DSC curves, respectively.

The relationship between temperature T and time t is given by Eq. (3) during the non-isothermal crystallization process, as follows:

$$t = \frac{|T_0 - T|}{D}, \tag{3}$$

where t is the crystallization time, T_0 the temperature at which crystallization begins ($t = 0$), T the temperature at a crystallization time, and D is the cooling rate.

In this study, the samples of B2 and B3, shown with only one exothermic peak in DSC curves, are selected to study their non-isothermal crystallization kinetics. The non-isothermal crystallization exothermic peaks of B2 and B3 blends at various cooling rate, D, are shown in Fig. 5. The parameters of non-isothermal crystallization are summarized in Table 2. The exothermic peak temperature, T_p, shifts to lower temperature region with increasing cooling rates. From the DSC digital information, the relative crystallinity (X_t) is calculated at different temperature T, and the plots of X_t versus T are shown in Fig. 6(a and b).

According to Eq. (3) the horizontal T-axis in Fig. 6 can be transformed into the crystallization time t-axis as shown in Fig. 7. It can be seen from Fig. 7 that all these curves have similar sigmoidal shape, and the curvature of the upper parts of the plot is observed to be level off due to the spherulites impingement that already begin from the inflection point of the curves. The characteristic sigmoidal curves are shifted to lower temperature or shorter time with increasing cooling rates for completing the crystallization. Through Fig. 7(a and b), we can get the half time of crystallization, $t_{1/2}$, when the X_t are equal to 50%, and the parameters are listed in Table 2. It can be seen

Table 2
Parameters of non-isothermal crystallization analyzed by Avrami theory for B2 and B3 blends

D (°C/min)	B2						B3					
	T_p (°C)	$t_{1/2}$ (s)	n	X_t (%)	K_c (10^{-4} s^{-n})	ΔH (J/g)	T_p (°C)	$t_{1/2}$ (s)	n	X_t (%)	K_c (10^{-4} s^{-n})	ΔH (J/g)
5	210.3	325.4	6.0	59.4	3	−35.4	207.24	287.0	5.7	53.3	15	−39.248
10	205.8	188.2	5.9	56.1	446	−34.8	201.21	164.9	5.5	57.6	607	−36.771
15	203.2	124.1	5.2	60.0	1672	−34.3	197.33	118.4	5.4	61.7	1757	−36.085
20	199.6	94.3	4.5	64.7	2688	−31.5	194.62	83.7	5.3	62.0	2902	−33.652

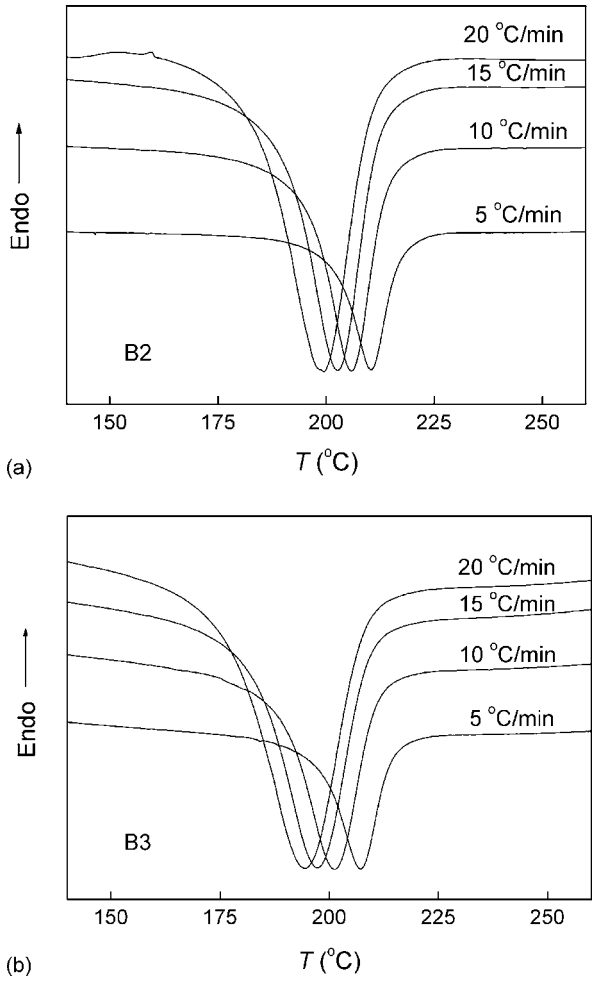

Fig. 5. Non-isothermal crystallization curves of (a) B2 and (b) B3 blends at different cooling rates.

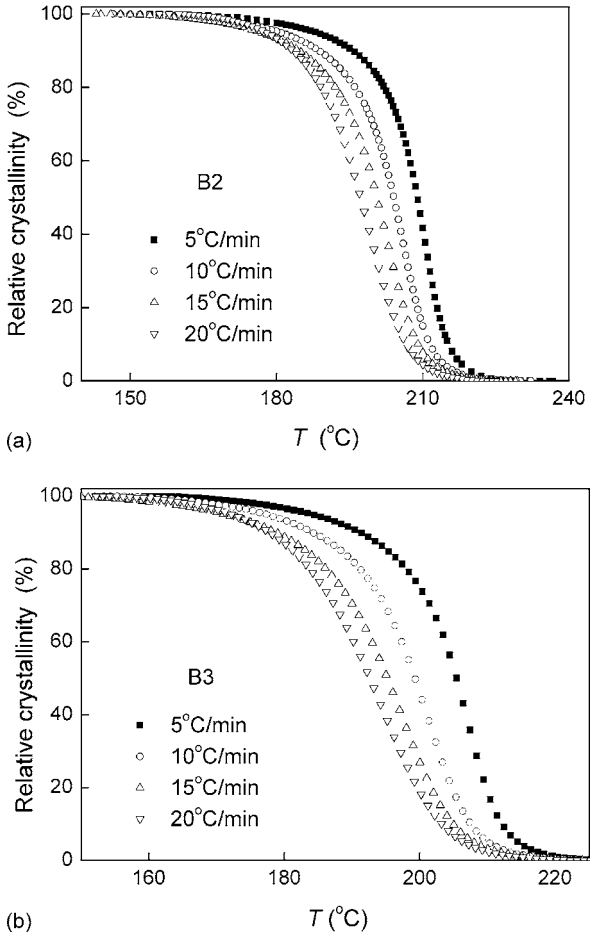

Fig. 6. Relative crystallinity vs. temperature for non-isothermal crystallization of (a) B2 and (b) B3 blends.

that $t_{1/2}$ values decrease with increasing cooling rates, indicating a progressively faster crystallization rate as the cooling rate increases. Moreover, compared the values of $t_{1/2}$ of B2 with that of B3 at a given cooling rate, it is clear that the more the PTT component in binary blend, the lower the $t_{1/2}$, and the higher the crystallization rate is.

Mandelkern [25] considered that the primary stage of non-isothermal crystallization could be described by Avrami equation [26,27], based on the assumption that the crystallization temperature is constant. Mandelkern obtained the following:

$$1 - X_t = \exp(-K_t t^n) \tag{4}$$

$$\log[-\ln(1 - X_t)] = n \log t + \log K_t \tag{5}$$

where K_t is a growth rate constant involving both nucleation and growth rate parameters. Jeziorny [28] considered the values of K_t determined by Avrami equation should be adequate as follows:

$$\log K_c = \frac{\log K_t}{D} \tag{6}$$

where K_c is the kinetic crystallization rate constant.

Fig. 8(a and b) show a series of double logarithm plot of $\log[-\ln(1 - X_t)]$ versus $\log t$ at different cooling rates. The Avrami exponent n and K_c of B2 and B3 are obtained from the slopes and the intercepts and listed in Table 2, respectively. Each curve in Fig. 8 shows good linearity except a secondary crystallization at the later crystallization stage. The values of X_t that the primary crystallization finishes or the secondary crystallization starts at given cooling rates are listed in Table 2 too. In this paper, the attention is focused on the primary crystallization.

The Avrami exponent n of the binary blend is found to range from 4.5 to 6.0 for B2, and 5.3 to 5.7 for B3 when cooling rate increased from 5 to 20 °C/min. This result of the values of exponent $n > 4$ at various cooling rates may due to the spherulites' impingement and crowding, or the complicated nucleation types and growth form of spherulites [29]. It is known that the nucleation mode is dependent on the cooling rate [30]. As seen from Table 2, the values of n decreased gradually with increasing of the cooling rate for each blend, indicating the crystallization growth is on fewer dimensions with increasing cooling rate. The values of the K_c gradually increase with increasing of cooling rates. As it is well known, higher cooling rate results in lower T_p, which in turn results in higher super-cooling. Thus, crystallization rates are enhanced. Moreover, ΔH is gradually decreased due to the less crystallites formed in the blend with increasing cooling rate. Furthermore, compared the values of K_c and ΔH of B2 with those of B3 at a given cooling rate, it is suggested that the

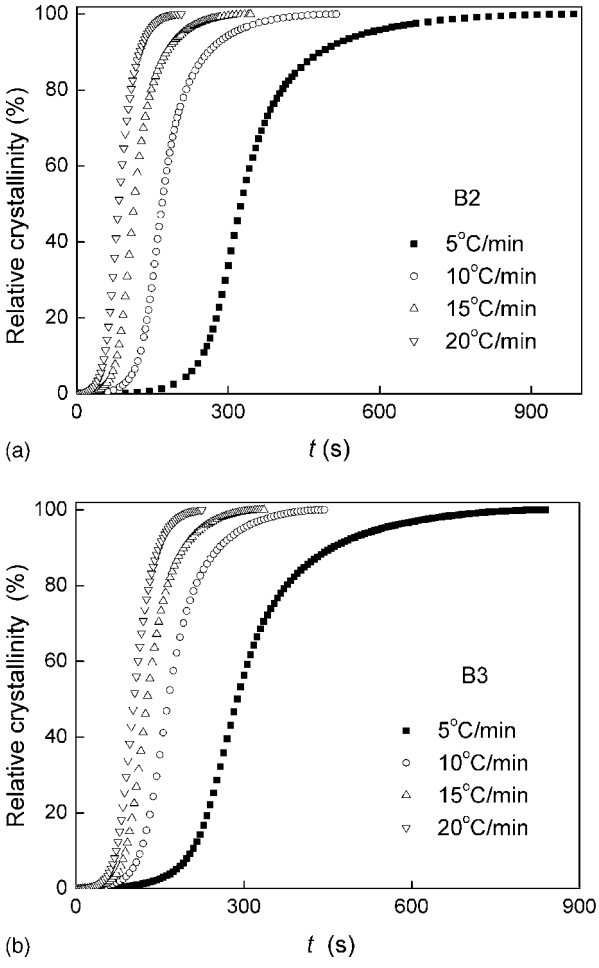

Fig. 7. Relative crystallinity vs. time for non-isothermal crystallization of (a) B2 and (b) B3 blends.

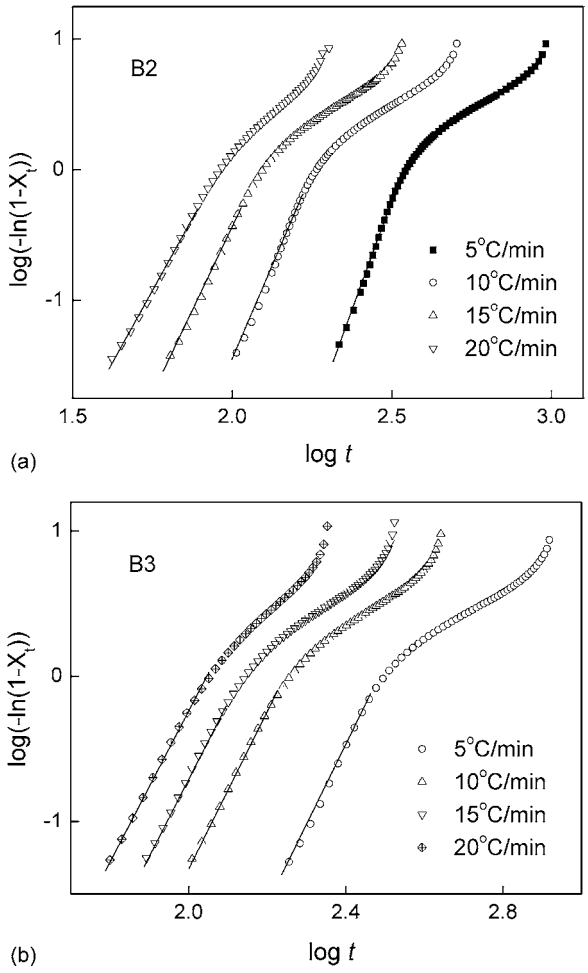

Fig. 8. Plots of $\log[-\ln(1-X_t)]$ vs. $\log t$ for non-isothermal crystallization of (a) B2 and (b) B3 blends.

binary blend with more PTT content has a higher crystallization rate and crystallinity than the less one.

3.3.2. Analysis based on the Ozawa theory

Since the non-isothermal crystallization is a rate-dependent process, Ozawa [31] took into account the effect of cooling (or heating) rate, D, on the crystallization process from the melt or glassy state, and modified the Avrami equation as follows:

$$1 - X_t = \exp\left[-\frac{K(T)}{|D|^m}\right], \quad (7)$$

$$\log[-\ln(1 - X_t)] = \log K(T) - m \log D \quad (8)$$

where $K(T)$ is a function related to the overall crystallization rate that indicates how fast crystallization proceeds, and m is the Ozawa exponent that depends on the dimension of crystals growth. According to Ozawa's theory and plots of $\log[-\ln(1-X_t)]$ versus $\log D$ at a given temperature, a series of straight lines will be obtained if Ozawa analysis is valid, and the crystallization kinetic parameters m and $\log K(T)$ can be derived from the slope and the intercept, respectively.

The result of the Ozawa analysis for B2 and B3 blends are shown in Fig. 9(a and b), where a series of straight lines are obtained, and the value of m and $\log K(T)$ are listed in Table 3. For each blend, the values of m and $\log K(T)$ are increased with the increasing temperature indicating that the crystallization growth is on more dimensions and at fast crystallization rate at higher temperature, while it is on less dimensions and lower crystallization rate at lower temperature. Therefore, an accurate analysis for B2 and B3 blends of non-isothermal crystallization data could be performed with the Ozawa theory. Furthermore, compared

Table 3
Non-isothermal crystallization kinetic parameters analyzed by Ozawa equation for B2 and B3 blends

B2				B3			
T (°C)	m	$\log K(T)$	r^2	T (°C)	m	$\log K(T)$	r^2
190	0.40	0.74	0.9983	186	0.53	0.83	0.9913
192	0.45	0.74	0.9973	188	0.59	0.84	0.9891
194	0.50	0.75	0.9958	190	0.67	0.87	0.9869
196	0.57	0.76	0.9938	192	0.77	0.91	0.9857
198	0.67	0.79	0.9911	194	0.89	0.96	0.9872
200	0.79	0.84	0.9889	196	1.04	1.02	0.9885
202	0.96	0.90	0.9887	198	1.20	1.07	0.9935
204	1.17	0.98	0.9915	200	1.37	1.12	0.9968
206	1.41	1.04	0.9959	202	1.53	1.14	0.9993
208	1.62	1.05	0.9992	204	1.67	1.11	0.9988

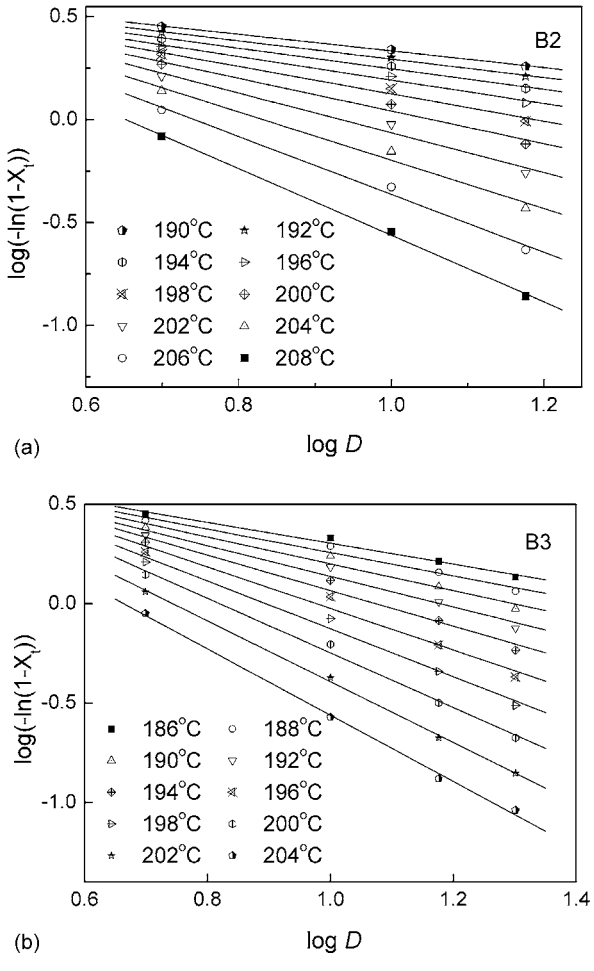

Fig. 9. Ozawa plots of $\log[-\ln(1-X_t)]$ vs. $\log D$ for (a) B2 and (b) B3 blends.

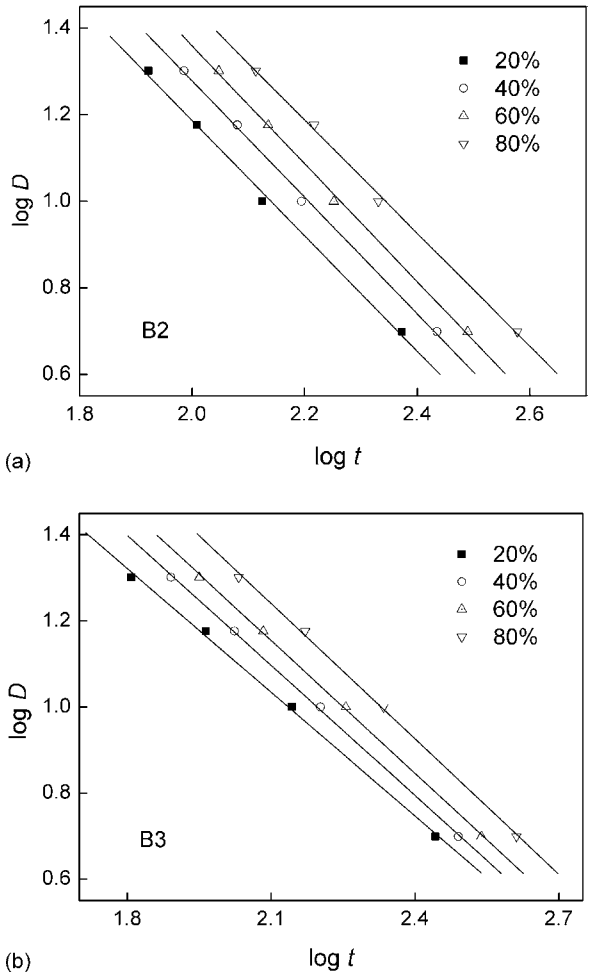

Fig. 10. $\log D$ vs. $\log t$ from the Mo equation for (a) B2 and (b) B3 blends.

the values of m and $\log K(T)$ of B2 with those of B3 in the temperature range of 190–204 °C, it is obvious that the results of B3 is higher than those of B2, indicating that the more PTT component in binary blends, the higher the crystal growth dimension and the crystallization rate are.

3.3.3. Analysis based on the Mo theory

Mo and co-workers [29] proposed a different kinetic equation by combining the Avrami and Ozawa equations. As the degree of crystallinity is related to the cooling rate D and the crystallization time t (or T), the relationship between D and t could be defined for a given degree of crystallinity. Consequently, a new kinetic equation for non-isothermal crystallization was derived by combining Eqs. (5) and (8):

$$\log K_t + n\ \log t = \log K(T) - m\ \log D \tag{9}$$

$$\log D = \log F(T) - b\ \log t \tag{10}$$

where the parameters $F(T) = [K(T)/K_t]^{1/m}$, and b is the ratio between the Avrami and Ozawa exponents, i.e. $b = n/m$. $F(T)$ refers to the value of cooling rate chosen at unit crystallization time when the system amounted to a certain degree of crystallinity. The smaller the value of $F(T)$ is, the higher the crystallization rate becomes. Therefore, $F(T)$ has a definite physical and practical meaning.

According to Mo's method, and plots of $\log D$ against $\log t$ at a given crystallinity will give a straight line with an intercept of $\log F(T)$ and a slope of $-b$ if Mo analysis is valid. As shown in Fig. 10, plotting $\log D$ against $\log t$ for B2 and B3 blends demonstrates linear relationship at a given X_t, and the values of $\log F(T)$ and b are listed in Table 4. $\log F(T)$ values are increased with the relative crystallinity from 3.81 to 4.04 (for B2) and 3.08 to 3.45 (for B3), indicating a lower crystallization rate is needed to reach the given crystallinity within unit time. The parameter b shows only a small increase with increasing X_t, ranging from 1.31 to 1.35 (for B2) and 1.01 to 1.09 (for B3), respectively. Compared the values of $\log F(T)$ of B2 with those of B3 at a given X_t, it is obvious that the results of B3 are lower than those of B2, indicating that the more the PTT content, the

Table 4
Non-isothermal crystallization kinetic parameters for B2 and B3 blends at given relative crystallinity analyzed by Mo equation

X_t(%)		20	40	60	80
B2	b	1.31	1.33	1.35	1.35
	$\log F(T)$	3.81	3.99	4.02	4.04
B3	b	1.01	1.03	1.05	1.09
	$\log F(T)$	3.08	3.23	3.32	3.45

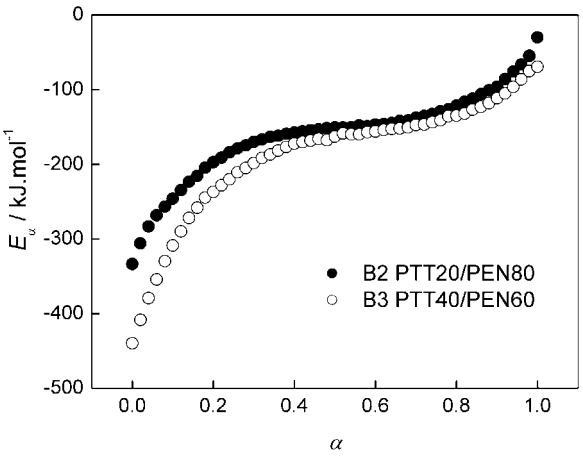

Fig. 11. Dependence of the effective activation energy on the crystallization conversion extent for two binary blends.

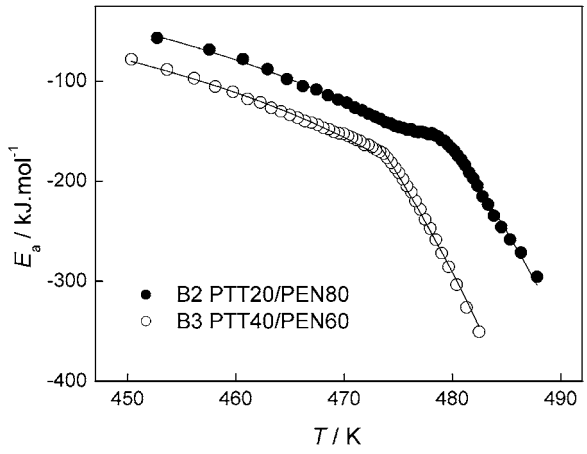

Fig. 12. Dependence of the effective activation energy on average temperature. The solid lines represent fits of Eq. (12).

higher the crystallization rate is. This conclusion is confirmed with those derived from the analysis from Avrami and Ozawa theory. Thus, the equation of Mo method successfully describes the non-isothermal crystallization process of the binary blends on the whole crystallization process.

3.3.4. Crystallization activation energy

In order to obtain the reliable values of the effective activation energy on the melt cooling process, Friedman [32] and Vyazovkin [33,34] developed differential iso-conversional method and advanced iso-conversional method, respectively. In this paper, the advanced iso-conversional method has been used to evaluate the effective activation energies as shown in Eq. (11):

$$\Phi(E_a) = \sum_{i=1}^{n}\sum_{j\neq i}^{n} \frac{J[E_a, T_i(t_a)]}{J[E_a, T_j(t_a)]} \tag{11}$$

where

$$J[E_a, T_i(t_a)] \equiv \int_{t_{a-\Delta a}}^{t_a} \exp\left[\frac{-E_a}{RT_i(t)}\right] dt \tag{12}$$

In Eq. (12), a varies from a to $1-\Delta a$ with a step $\Delta a = m^{-1}$, where m is the number of intervals chosen for analysis and it is set as $m = 50$ in this calculation. Fig. 11 shows the dependence of the effective activation energy on the extent of crystallization conversion of B2 and B3 blends. To each blend, the effective activation energy increases with the extent of the crystallization conversion, e.g. the effective activation energy increases from −333 to −30 kJ/mol for B2 blend and from −439 to −70 kJ/mol for B3 blend as the crystallization conversion increasing from 0 to 1. This result suggests that it is easier for blend to crystallize at the beginning of the crystallization, while it becomes difficult as the crystallization proceeding. By comparing the effective activation energy at the same extent of crystallization conversion, it is easy to find that the E_a of B3 blend is more negative than that of B2 blend, which indicates that the binary blend with more PTT component has higher crystallization ability than that with less PTT content. Therefore, PTT content improves the crystallization ability of PEN.

Because of the same value of a can be accomplished at different temperatures at various cooling rates, the average temperature is used to associate with a and the effective activation energy, thus, E_a on a dependence can be converted into the E on T dependence as presented in Fig. 12. As shown in Fig. 12, the $E_a(T)$ is decreased with increasing temperature, indicating easier crystallization occurs at higher temperature. Compared the value of E_a of B2 with those of B3 at the same temperature, it is clear that the more PTT content in blend, the higher crystallization ability is. Furthermore, the E_a dependence displays a breakpoint at 477 K for B2 and 474 K for B3 blend, which may be due to the change in crystallization mechanism. Subject to the change in crystallization mechanism, it makes sense to parameterize the higher temperature and lower temperature portions of the $E_a(T)$ dependence separately. The two portions of the $E_a(T)$ dependence have been fit to Eq. (13) derived by Vyazovkin [35,36] that has been accomplished by using graphics software Origin 7.0.

$$E_a(T) = U^* \frac{T^2}{T - T_\infty} + K_g R \frac{T_m^2 - T^2 - T_m T}{(T_m - T)^2} \tag{13}$$

the values of K_g and U^* yielded has been shown in Table 5.

Table 5
Crystallization parameters of B2 and B3 blends

Sample	T_∞ (K)	T_m (K)	I, III			II		
			U^* (kJ/mol)	$K_g \times 10^{-5}$ (K^2)	r^2	U^* (kJ/mol)	$K_g \times 10^{-5}$ (K^2)	r^2
B2	367	570	11.56	6.1	0.99	3.67	2.6	0.97
B3	355	570	9.89	6.3	0.99	0.38	3.5	0.98

From Table 5, the values of K_g for higher and lower temperature are 6.1×10^5 K^2 and 2.6×10^5 K^2 for B2 and 6.3×10^5 K^2 and 3.5×10^5 K^2 for B3 blend, respectively. The ratios of K_g for higher and lower temperature are 2.4 for B2 and 1.8, respectively. These values are very close to the theoretical ratio value 2, which corresponds to the change from regime I to regime II [37]. Compared the K_g of B2 with that of B3 at higher or lower temperature, it is apparent the more PTT content in binary blend, the faster crystallization rate is.

The value of the U^* at regime I (11.56 kJ/mol for B2, 9.89 kJ/mol for B3) is lager than that at regime II (3.67 kJ/mol for B2, 0.38 kJ/mol for B3). Although the U^* is usually set to be constant value (6.3 kJ/mol), Hoffman et al. [37] thought the best fits value of U^* tends to vary between 4.2 and 16.7 kJ/mol.

4. Conclusion

PTT/PEN binary blends prepared by melt-compound are investigated using differential scanning calorimeter and the results demonstrate different crystallization and melting behaviors with varied content of PTT in blends. All of the samples are miscible in amorphous phase by exhibiting a single glass-transition temperature. The values of T_g decreases gradually with increasing of PTT content and is described by Gordon–Taylor equation, the fitting parameter k is determined to be 0.31. A single exotherm is observed at higher temperature in the DSC curve when the ratio of PTT is less than 50% (w/w), suggesting that the crystallization of PEN component is improved by the minor component PTT; while the crystallization of PTT is obscured by PEN. With the increasing of PTT component to more than 50% (w/w), the exotherms of the binary blend exhibit two crystallization peaks, and both PTT and PEN components in the blends crystallized individually. There are one (for B2 and B3) or two (for B4 and B5) melting thermograms for the binary blends, which are corresponding to the melt of the crystals of PTT at lower temperature and PEN at higher temperature, respectively.

At the primary stage of the non-isothermal crystallization process of B2 and B3, the Avrami exponent, n is larger than 4; indicating that the crystallization process of the binary blend is more complicated than pure polymer. The Ozawa equation and the method developed by Mo are also successful in describing the non-isothermal crystallization process of the binary blends. Compared with B2 and B3 of the kinetic parameters, such as the Ozawa exponent m and the crystallization rate $\log K(T)$, or the $\log F(T)$, it is suggested that B3 has more crystal growth dimensions and higher crystallization rate than those of B2. Moreover, the effective activiation energy calculated by advanced isoconversional method suggests that the binary blend with more PTT component has higher crystallization ability than that with less PTT content. The value of E_a depends not only on the system but also on T. The Hoffman–Lauritzen parameters (U^* and K_g) of the B2 and B3 blends are determined from the overall rate of the non-isothermal crystallization, respectively.

References

[1] J.R. Whinfield, J.T. Dickson, British Patent 578,079, June 14, 1946.
[2] J. Wu, J.M. Schultz, J.M. Samon, A.B. Pangelinan, H.H. Chuah, Polymer 42 (2001) 7141.
[3] J.A. Grande, Mod. Plast. 12 (1997) 97.
[4] K. Nakamae, T. Nishino, K. Tada, T. Kannamoto, M. Ito, Polymer 34 (1993) 3322.
[5] C.J.M. Van Den Heuvel, E.A. Klop, Polymer 41 (2000) 4249.
[6] Y. Uchida, Nikkei Mater. Technol. 137 (1994) 63.
[7] Naphthalates-Film Applications. http://www.bp.com/liveassets/bp_internet/globalbp/STAGING/global_assets/downloads/pdfs/acetyls_aromatics_pta/N_16_Film.pdf.
[8] J. Myers, Mod. Plast. 70 (1993) 42.
[9] K.H. Yoon, S.C. Lee, O.O. Park, Polym. Eng. Sci. 35 (1995) 1807.
[10] Y. Yu, K.J. Choi, Polym. Eng. Sci. 37 (1997) 91.
[11] P. Supaphol, N. Dangseeyun, P. Thanomkiat, M. Nithitanakul, J. Polym. Sci. Polym. Phys. 42 (2004) 676.
[12] N. Dangseeyun, P. Supaphol, M. Nithitanakul, Polym. Test 23 (2004) 187.
[13] S.P. Rwei, Polym. Eng. Sci. 39 (1999) 2475.
[14] P. Krutphun, P. Supaphol, Eur. Polym. J. 41 (2005) 1561.
[15] J.C. Ho, T.C. Lin, K.H. Wei, Polymer 41 (2000) 9299.
[16] J.P. Penning, R. Manley, Macromolecules 29 (1996) 77.
[17] P. Xing, X. Ai, L. Dong, Z. Feng, Macromolecules 31 (1998) 6898.
[18] M. Gordon, J.S. Taylor, J. Appl. Chem. 2 (1952) 493.
[19] T.G. Fox, Bull. Am. Phys. Soc. 2 (1956) 123.
[20] Y. Shi, S.A. Jabarin, J. Appl. Polym. Sci. 81 (2001) 11.
[21] S.B. Lin, J.L. Koenig, J. Polym. Sci. Polym. Symp. 71 (1984) 121.
[22] K.H. Wei, H.C. Jang, J.C. Ho, Polymer 38 (1997) 3521.
[23] J.P. Penning, R. Manley, Macromolecules 29 (1996) 77.
[24] D.S. Park, S.H. Kim, J. Appl. Polym. Sci. 87 (2003) 1842.
[25] R.A. Fava, Methods of Experimental Physics, Academic Press, New York, 1980.
[26] M. Avrami, J. Chem. Phys. 8 (1940) 212.
[27] M. Avrami, J. Chem. Phys. 7 (1936) 1103.
[28] A. Jeziorny, Polymer 19 (1978) 1142.
[29] M.Y. Liu, Q.X. Zhao, Y.D. Wang, C.G. Zhang, Z.S. Mo, S.K. Cao, Polymer 44 (2003) 2537.
[30] C.R. Choe, K.H. Lee, Polym. Eng. Sci. 29 (1989) 801.
[31] T. Ozawa, Polymer 12 (1971) 150.
[32] H. Friedman, J. Polym. Sci. C6 (1964–1965) 183.
[33] S. Vyazovkin, J. Comput. Chem. 18 (1997) 393.
[34] S. Vyazovkin, J. Comput. Chem. 22 (2001) 178.
[35] S. Vyazovkin, N. Sbirrazzuoli, Macromol. Rapid Commun. 25 (2004) 733.
[36] S. Vyazovkin, D. Ion, Macromol. Chem. Phys. 207 (2006) 20.
[37] J.D. Hoffman, G.T. Davis, J.I. Lauritzen Jr., in: N.B. Hannay (Ed.), Treatise on Solid State Chemistry, vol. 3, Plenum, NY, 1976, p. 479.